

Effects of simulated natural variability on Arctic temperature projections

Asgeir Sorteberg,¹ Tore Furevik,^{2,3} Helge Drange,^{3,4,5,6} and Nils Gunnar Kvamstø^{2,3}

Received 3 May 2005; revised 28 June 2005; accepted 15 August 2005; published 23 September 2005.

[1] A five-member ensemble with a coupled atmosphere-sea ice-ocean model is used to examine the effects of natural variability on climate projections for the Arctic. The individual ensemble members are initialized from a 300 years control experiment, each starting from different strengths and phases of the Atlantic Meridional Overturning Circulation. The ensemble members are integrated for 80 years with a 1% per year increase in the atmospheric concentration of CO₂. The main findings are that on decadal time scales, multi-model spread of estimated temperature changes in the Arctic may potentially be attributed to internal variability of the climate system. During weak CO₂ forcing the internal variability may mask the strength of the anthropogenic signals for several decades. The implications of the findings are that attribution of any Arctic climate change trends calculated over a few decades is difficult.
Citation: Sorteberg, A., T. Furevik, H. Drange, and N. G. Kvamstø (2005), Effects of simulated natural variability on Arctic temperature projections, *Geophys. Res. Lett.*, 32, L18708, doi:10.1029/2005GL023404.

1. Introduction

[2] The northern high latitudes have for many years been recognized as the region most sensitive to anthropogenic climate change, with projected temperature changes being typically 2 times larger than the global mean change [e.g., *Intergovernmental Panel on Climate Change (IPCC)*, 2001; *Holland and Bitz*, 2003; *Hu et al.*, 2004, *McBean*, 2005]. Due to the low moisture content, changes in greenhouse gasses have the potential to become more important in the Arctic than at lower latitudes. In addition the complicated interaction between the atmosphere, ocean and cryosphere give rise to a variety of climate feedbacks as such as ice-albedo and cloud feedbacks. The direct effect of the ice-albedo feedback is that anomalous melting of snow and ice reduces the albedo and thus increases the absorption of incoming solar radiation [e.g., *Manabe and Stouffer*, 1980; *Curry et al.*, 1995]. For the latter, enhanced evaporation from more open water leads to increased cloud amount and increased long-wave radiation to the surface [e.g., *Curry et al.*, 1996]. The cloud effect strongly depends on season and

cloud type. Measurements during the SHEBA program [*Uttal et al.*, 2002] indicated a cloud-induced surface warming throughout most of the year, with long-wave climate sensitivity being close to 0.65 W m⁻² per percent change in cloudiness [*Shupe and Intrieri*, 2004].

[3] Less known are the potential dynamical feedbacks that may be associated with global warming. Most model simulations suggest a general decrease in the meridional oceanic heat transport south of 60°N, and a slight increase poleward of this latitude [*Covey et al.*, 2003]. The inter-model differences are, however, substantial. For the large-scale atmospheric circulation the uncertainties are even larger, although there is a tendency for a strengthening of the North Atlantic westerlies in many of the model simulations [*Osborn*, 2004; *Kuzmina et al.*, 2005].

[4] *Randall et al.* [1998] point out that poor understanding of key physical processes in the region causes a considerable part of the uncertainty associated with Arctic climate projections. In atmosphere, the most critical processes are turbulent transport in stable boundary layers, radiation, cloud formation, and complex interactions among them. Central processes in the ocean are freezing and melting of sea-ice, sea-ice dynamics, turbulent mixing in the upper part of the water column, and the poleward transport of heat. The lack of process knowledge and process interactions has led to a variety of numerical formulations and parameterizations. This in turn has produced a wide spread in the representations of present day control climate and responses to anthropogenic forcing [*IPCC*, 2001; *Räisänen*, 2001].

[5] A second kind of uncertainty is related to the large internal variability at high latitudes. An example of such variability is the early warming of the 1930s and 1940s, which, although primarily an Arctic mode, was sufficiently strong to show up in globally averaged temperature compilation [*Bengtsson et al.*, 2004]. Since natural variability will add “noise” to the climate signal, averaging over a long time period or over many model realizations is necessary to get statistically reliable estimates of human-induced climate change signals.

[6] The use of sufficiently long averaging time periods is, however, problematic for many observational-based time series since these are in general short, especially in the Arctic. An additional complication is that the 20th century anthropogenic climate forcing has given climate responses that are still weak and comparable to the amplitude of the natural climate variability modes. Climate models and increasing availability of computational resources can, however, be used as a laboratory to explore how the signal-to-noise ratio varies as function of averaging time and strength of the signal.

[7] In this study we quantify the uncertainties related to insufficient sampling of internal variability of the Arctic

¹Bjerknes Centre for Climate Research, University of Bergen, Bergen, Norway.

²Geophysical Institute, University of Bergen, Bergen, Norway.

³Also at Bjerknes Centre for Climate Research, University of Bergen, Bergen, Norway.

⁴Nansen Environmental and Remote Sensing Center, Bergen, Norway.

⁵Also at Geophysical Institute, University of Bergen, Bergen, Norway.

⁶Also at Nansen-Zhu International Research Centre, Beijing, China.

surface temperature based on results from ensemble simulations with a numerical coupled atmosphere-sea ice-ocean climate model.

[8] In section 2 the methodology and experimental setup of the model system are described. The projected Arctic temperature changes in the model ensemble are presented in section 3, and discussed in section 4. In section 5 the paper is summarized with the main findings and the implications for Arctic climate projections.

2. Model Description and Analysis Methods

[9] The numerical model used is the Bergen Climate Model (BCM) [Furevik *et al.*, 2003]. It consists of the global atmospheric model ARPEGE/IFS [Déqué *et al.*, 1994] and a global version of the ocean model MICOM [Bleck *et al.*, 1992], the latter including a dynamic and thermodynamic sea-ice model based on Semtner [1976] thermodynamics and Hibler [1979] rheology. In this version of BCM, ARPEGE/IFS uses a spectral truncation at wave number 63 with a horizontal grid mesh of about 2.8° by 2.8° and 31 vertical levels from surface to 10 hPa. MICOM is set up with a horizontal resolution of approximately 2.4° by 2.4° with 24 layers in the vertical. The horizontal resolution in the ocean increases towards the two model poles located over Siberia and Antarctica. To resolve the equator-confined dynamics, the meridional resolution gradually increases to 0.8° in the tropics. In order to avoid drift from climatology, the heat and fresh water fluxes are modified based on seasonally varying flux-adjustment terms derived from the spin-up of the model.

[10] A detailed description of the technical details and performance of the BCM system is given by Furevik *et al.* [2003]. In addition, detailed descriptions of the simulated North Atlantic Oscillation (NAO) and the Atlantic Meridional Overturning Circulation (AMOC) variability modes are presented by Kuzmina *et al.* [2005] and Bentsen *et al.* [2004], respectively.

[11] A five-member ensemble has been generated based on initial conditions taken from a 300-year control integration. Except for a 1% per year increase in atmospheric CO_2 , the atmospheric constituents and aerosols are kept constant in the ensemble integrations. This is the same kind of experiment as carried out in the second phase of the Coupled Model Intercomparison Project (CMIP2) [Meehl *et al.*, 2000; Covey *et al.*, 2003]. As the strength of AMOC and the associated northward heat transport by the ocean have most energy on decadal to inter-decadal time scales [e.g., Bentsen *et al.*, 2004; Collins *et al.*, 2005], each of the ensemble members are chosen to start at different phases of the AMOC in the control integration (Figure 1). This ensures a larger spread in initial conditions than what is achieved by the traditional method in which the atmosphere state is slightly perturbed around a fixed and in general an arbitrary chosen, ocean state.

3. Projected Changes in the Arctic Climate

[12] The linear trends in the zonal-mean temperature, taken over the full integration length (80 years) of the BCM ensemble members shows a strong polar amplification, with a typical warming of $0.5\text{--}1.2^\circ\text{C}/\text{decade}$ at high

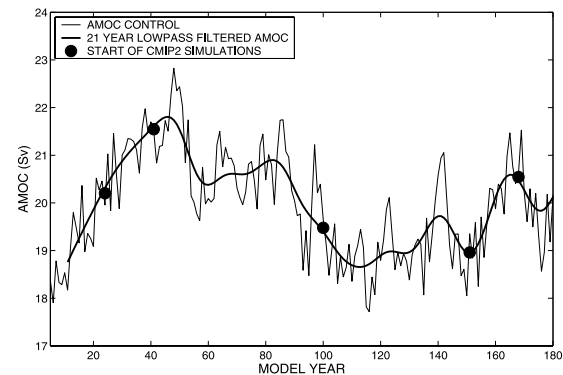


Figure 1. Maximum strength of the AMOC from the BCM control run (solid) and 21-year lowpass filtered values (solid, bold). The bullets indicate the starting points of the five ensemble members.

northern latitudes (Figure 2a). Comparing the single-model BCM ensemble with the 15-model ensemble in CMIP2, the former shows less than average warming in the 30°N to 40°N latitude band, but stronger warming than the CMIP2 ensemble mean in the Arctic.

[13] Qualitatively, a measure for the internal variability of a system is the spread between the various members of an ensemble. Comparing the BCM spread with the CMIP2 spread over the first 25 years of the perturbation experiments (representing a CO_2 forcing up to 35% higher than the present day level), the northern latitude spread of BCM is almost as large as the CMIP2 spread and twice as large as the average temperature change (or warming signal) (Figure 2b). Thus over the first 25 years of the perturbation experiments, the signal-to-noise ratio is very low, and it is therefore difficult to separate an anthropogenic signal from internal climate variability.

[14] In the tropics and subtropics the spread among the various BCM members is much less than the multimodel spread, while the southern ocean and Antarctica are characterized by a small warming signal and a large spread.

[15] The regional distribution of the warming signal show strongest change between Greenland and the North Pole and in the northern Kara Sea, where the temperature increase over the 80 year period exceeds $1^\circ\text{C}/\text{decade}$ (Figure 3a). This is the area where the sea-ice cover in the control run has maximum thickness [Furevik *et al.*, 2003]. Typical warming over the northernmost continental areas is of the order of $0.5\text{--}0.7^\circ\text{C}/\text{decade}$. The spread among the various BCM members is typically between 0.1 and $0.2^\circ\text{C}/\text{decade}$, with lowest values over the continents and highest values in the areas showing the strongest warming signal. Typically the warming signal is 3 times the spread.

[16] Comparing the warming signal from year 1–25 with years 1–80, it is seen that the pattern is similar, but with strongest warming north of the Canadian Archipelago and in the northeastern Barents Sea, with values being $0.6\text{--}0.9^\circ\text{C}/\text{decade}$ over the Arctic Ocean. The spread among the ensemble members is larger than the warming signal over most of the Arctic with a maximum spread over the central Arctic where it exceeds $2^\circ\text{C}/\text{decade}$. As seen in Figure 1, this indicates that there is no consensus among the ensemble

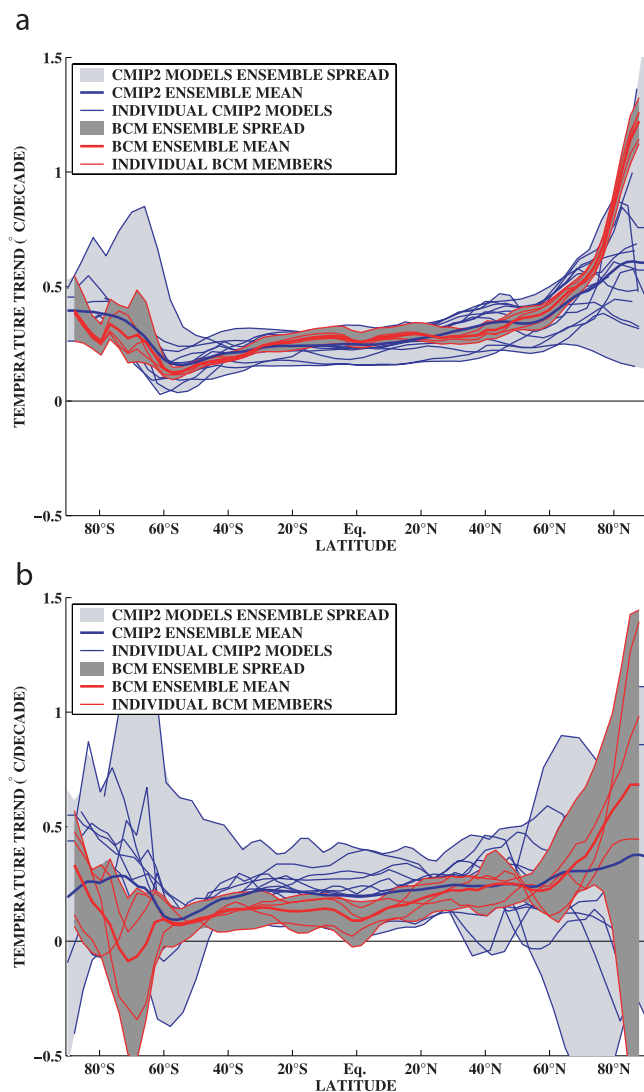


Figure 2. (a) Zonal-mean 2 m temperature trends ($^{\circ}\text{C}/\text{decade}$) as simulated by the CMIP2 and BCM ensembles over years 1–80. Trends in control integrations have been subtracted. Light shading is the spread of the CMIP2 members [e.g., *Hu et al.*, 2004]; dark shading is the spread of the BCM ensemble. The thick blue (red) curve shows the ensemble mean of the CMIP2 (BCM) members, and the thin blue (red) curves the individual CMIP2 (BCM) ensemble members. (b) Same as Figure 2a but for years 1–25.

members on the sign of the Arctic temperature trend over this time period.

4. Discussion

[17] All of the BCM ensemble members show strong warming in the high northern latitudes when trends are calculated over the whole 80 year time period. The main reason for this is a realistically distributed but too thin sea-ice cover in the control run [*Furevik et al.*, 2003] that melts when the greenhouse gas forcing increases. The melted sea-ice exposes the Arctic atmosphere to relatively warm open waters instead of a perennial ice cover [see *Holland and Bitz*, 2003; *Hu et al.*, 2004].

[18] Another feature of BCM compared to the CMIP2 integrations is a reduced warming signal at 30°N to 40°N (not shown). An explanation for this is a substantial strengthening of the NAO in BCM [see *Kuzmina et al.*, 2005], shifting the North Atlantic drift eastwards leading to colder sea surface temperatures in this region. This process reduces the warming in the Northwest Atlantic and enhances the warming of the Nordic Seas [e.g., *Otterå et al.*, 2004]. Other models with a strengthened NAO show similar features with a cold northwest Atlantic and a warm Arctic [cf. *Holland and Bitz*, 2003; *Kuzmina et al.*, 2005].

[19] The spread among the various CMIP2-models in Figure 2 implies large uncertainty in the climate projections, and consequently in any climate impact assessments, of the Arctic. As demonstrated by the five-member BCM ensemble, any trend estimates taken over a few decades are subject to large uncertainties due to internal variability of the climate system. As long as the number of years used in the trend estimates are the same the ratio between the BCM spread and multimodel ensemble spread is relatively constant regardless of starting point. For example the mean

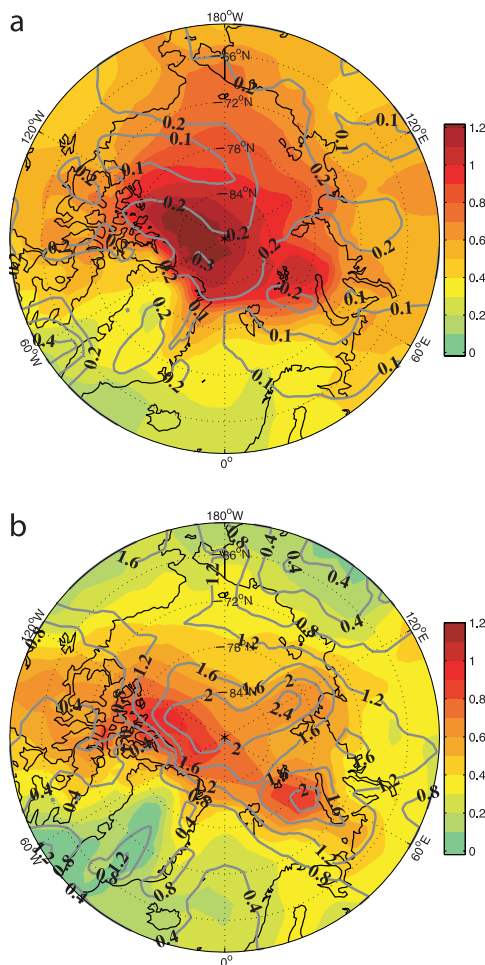


Figure 3. (a) Projected Arctic temperature trends over years 1–80 and (b) years 1–25. Color shading indicates ensemble-mean 2 m temperature trends ($^{\circ}\text{C}/\text{decade}$), and solid lines show the spread in trends among the various ensemble members (contour interval is 0.1 and $0.4^{\circ}\text{C}/\text{decade}$ for Figures 3a and 3b, respectively).

ratio between the BCM and multimodel spread over the latitudinal bands north of 60°N was 40–60% for trends calculated over different 25 year periods (year 1–25, 25–50 and 50–75). Increasing the years used in the trend estimates from 25 to 50 reduced the spread among the BCM members by 30–40% and the spread is further reduced (over 70%) when all 80 years was used in the trend estimates (Figure 2b). The reduction in the multimodel spread is much less pronounced as different representations of the feedback processes in the climate models increases the multi-model spread.

5. Conclusion

[20] A 5-member ensemble of BCM, compared to a 15-member multi-model ensemble, is used to examine the effects of natural variability on climate projections for the Arctic. The main findings are:

[21] – When the changes in the external forcings are small a significant part of multi-model differences for climate projections for the Arctic may potentially be explained by internal climate variability and not necessarily real model differences

[22] – Internal climate variability may mask the strength of the anthropogenic signal for several decades.

[23] – Trend estimates exceeding the time scales of the leading low frequency internal climate variability modes, or trends over many model realizations, increases the signal-to-noise level and makes the climate projections considerably more robust against uncertainties related to insufficient sampling of internal variability.

The multi-model spread in estimated Arctic warming confirms the poor understanding of high latitude physical processes and their response. This represents a great challenge for observationalists, theoreticians and modelers alike in the years to come.

[24] It is important to realize that the trend estimates based on 25 years as in Figures 2b and 3b is comparable to the period with satellite observations of several Arctic climate variables, and it is also consistent with a common time horizon for societal and industry planning and decision making.

[25] Implications of the presented findings are that observed or simulated Arctic climate change trends calculated over a few decades may be strongly influenced by internal variability, making it hard to attribute the changes to any specific external forcings.

[26] **Acknowledgments.** The Research Council of Norway through RegClim, Macesiz, ROLARC, and the Programme of Supercomputing has supported the model development and analysis. The work has also received support from the EU-project ENSEMBLES (GOCE-CT-2003-505539). This is contribution A99 from the Bjerknes Centre for Climate Research.

References

Bengtsson, L., V. A. Semenov, and O. M. Johannessen (2004), The early twentieth-century warming in the Arctic—A possible mechanism, *J. Clim.*, *17*, 4045–4057.

Bentsen, M., H. Drange, T. Furevik, and T. Zhou (2004), Variability of the Atlantic thermohaline circulation in an isopycnal coordinate OGCM, *Clim. Dyn.*, *22*, 701–720, doi:10.1007/s00382-004-0397-x.

Bleck, R., C. Rooth, D. Hu, and L. T. Smith (1992), Salinity-driven thermohaline transients in a wind- and thermohaline-forced isopycnal coordinate model of the North Atlantic, *J. Phys. Oceanogr.*, *22*, 1486–1515.

Collins, M., et al. (2005), Interannual to decadal climate predictability: A multi-perfect-model-ensemble, *J. Clim.*, in press.

Covey, C., K. M. AchutaRao, U. Cubasch, P. Jones, S. J. Lambert, M. E. Mann, T. J. Phillips, and K. E. Taylor (2003), An overview of results from the Coupled Model Intercomparison Project, *Global Planet. Change*, *37*, 103–133.

Curry, J. A., J. L. Schramm, and E. E. Ebert (1995), Sea-ice albedo climate feedback mechanism, *J. Clim.*, *8*, 240–247.

Curry, J. A., W. B. Rossow, D. Randall, and J. L. Schramm (1996), Overview of Arctic cloud and radiation characteristics, *J. Clim.*, *9*, 1731–1764.

Déqué, M., C. Dreveton, A. Braun, and D. Cariolle (1994), The ARPEGE/IFS atmosphere model: A contribution to the French community climate modeling, *Clim. Dyn.*, *10*, 249–266.

Furevik, T., M. Bentsen, H. Drange, I. K. T. Kindem, N. G. Kvamstø, and A. Sorteberg (2003), Description and validation of the Bergen Climate Model: ARPEGE coupled with MICOM, *Clim. Dyn.*, *21*, 27–51.

Hibler, W. D., III (1979), A dynamic thermodynamic sea ice model, *J. Phys. Oceanogr.*, *9*, 815–846.

Holland, M. M., and C. M. Bitz (2003), Polar amplification of climate change in coupled models, *Clim. Dyn.*, *21*, 221–232.

Hu, Z.-Z., S. I. Kuzmina, L. Bengtsson, and D. M. Holland (2004), Sea-ice change and its connection with climate change in the Arctic in CMIP2 simulations, *J. Geophys. Res.*, *109*, D10106, doi:10.1029/2003JD004454.

Intergovernmental Panel on Climate Change (IPCC) (2001), *Climate Change 2001: The Scientific Basis: Contribution of Working Group I to the Third Assessment Report of the Intergovernmental Panel on Climate Change*, edited by J. T. Houghton et al., 881 pp., Cambridge Univ. Press, New York.

Kuzmina, S. I., L. Bengtsson, O. M. Johannessen, H. Drange, L. P. Bobylev, and M. W. Miles (2005), The North Atlantic Oscillation and greenhouse-gas forcing, *Geophys. Res. Lett.*, *32*, L04703, doi:10.1029/2004GL021064.

Manabe, S., and R. J. Stouffer (1980), Sensitivity of a global climate model to an increase of CO₂ concentration in the atmosphere, *J. Geophys. Res.*, *85*, 5529–5554.

McBean, G. A. (2005), Arctic climate—Past and present, in *Arctic Climate Impact Assessment (ACIA)*, Cambridge Univ. Press, New York, in press.

Meehl, G. A., F. Zwiers, J. Evans, T. Knutson, L. Mearns, and P. Whetton (2000), Trends in extreme weather and climate events: Issues related to the modeling extremes in projections of future climate change, *Bull. Am. Meteorol. Soc.*, *81*, 427–436.

Osborn, T. J. (2004), Simulating the winter North Atlantic Oscillation: The roles of internal variability and greenhouse gas forcing, *Clim. Dyn.*, *22*, 605–623.

Otterå, O. H., H. Drange, M. Bentsen, N. G. Kvamstø, and D. Jiang (2004), Transient response of enhanced freshwater to the Nordic Seas—Arctic Ocean in the Bergen Climate Model, *Tellus*, *56*, 342–361.

Räisänen, J. (2001), CO₂-induced climate change in CMIP2 experiments: Quantification of agreement and role of internal variability, *J. Clim.*, *14*, 2088–2104.

Randall, D., J. Curry, D. Battisti, G. Flato, R. Grumbine, S. Hakkinen, D. Martinson, R. Preller, J. Walsh, and J. Weatherly (1998), Status of and outlook for large-scale modelling of atmosphere-ice-ocean interactions in the Arctic, *Bull. Am. Meteorol. Soc.*, *79*, 197–219.

Semtner, A. J., Jr. (1976), A model for the thermodynamic growth of sea ice in numerical investigations of climate, *J. Phys. Oceanogr.*, *6*, 379–389.

Shupe, M. D., and J. M. Intrieri (2004), Cloud radiative forcing of the Arctic surface: The influence of cloud properties, surface albedo, and solar zenith angle, *J. Clim.*, *17*, 616–628.

Uttal, T., et al. (2002), Surface heat budget of the Arctic Ocean, *Bull. Am. Meteorol. Soc.*, *83*, 255–276.

H. Drange, Nansen Environmental and Remote Sensing Center, Thormøhlensgt. 47, N-5006 Bergen, Norway.

T. Furevik and N. G. Kvamstø, Geophysical Institute, University of Bergen, Allengaten 70, N-5007 Bergen, Norway.

A. Sorteberg, Bjerknes Centre for Climate Research, University of Bergen, Allengaten 55, N-5007 Bergen, Norway. (asgeir.sorteberg@bjerknes.uib.no)